İSTANBUL UNIVERSITY CERRAHPAŞA

ORIGINAL ARTICLE
Electrica 2025

A 4-Port Semi-Circular Arc Slotted MIMO Antenna for Sub-6 GHz 5G Automotive Wireless Communications

Ashish Kumar[1], Bikash Chandra Sahoo[2], Gurmeet Singh[3], Soumya Ranjan Mishra[2], Ashutosh Sharma[4], Rajeev Kumar[1]

[1]Chitkara University Institute of Engineering and Technology, Chitkara University, Punjab, India
[2]Department of ETC Engineering, Indira Gandhi Institute of Technology, Sarang, Odisha, India
[3]School of Computing Science and Engineering, Galgotias University, Greater Noida, India
[4]Business School, Henan University of Science and Technology, Luoyang, China

Cite this article as: A. Kumar, B. Chandra Sahoo, G. Singh, S. Ranjan Mishra, A. Sharma, and R. Kumar, "A 4-port semi-circular arc slotted MIMO antenna for sub-6 GHz 5G automotive wireless communications," *Electrica*, 25, 0150, 2025. doi: 10.5152/electrica.2025.24150.

WHAT IS ALREADY KNOWN ON THIS TOPIC?

- *In recent years, numerous antenna designs have been proposed for sub-6 GHz 5G applications, especially targeting automotive environments. Prior studies have established the effectiveness of MIMO (Multi-Input Multi-Output) configurations in enhancing channel capacity and reliability for vehicular communication. Antennas operating in the sub-6 GHz spectrum are particularly important due to their favorable propagation characteristics and compatibility with existing infrastructure.*
- *The proposed design exhibits the wide bandwidth covering the very low band*

Corresponding author: Rajeev Kumar,

E-mail:
Rajeev.kumar@chitkara.edu.in

Received: October 25, 2024
Revision Requested: January 5, 2025
Last Revision Received: April 21, 2025
Accepted: April 29, 2025
Publication Date: September 5, 2025

DOI: 10.5152/electrica.2025.24150

ABSTRACT

An antenna is designed in a multi-input multi-output configuration composed of four radiating elements embedded with semi-circular cuts for sub-6 GHz 5G automotive applications. The performance of the proposed design has been enhanced with the utilization of the concept of partial ground. The antenna covers the −10 dB impedance bandwidth in the frequency spectrum of sub-6 GHz, which includes 0.9 GHz, 3 GHz, and 4.7 GHz. The proposed design exhibits a wide bandwidth of 4.8 GHz, ranging from 0.7 GHz to 5.5 GHz with a peak gain of 8.8 dB in the resonating band. The isolation between the elements is well below −15 dB, and to maintain this high isolation, the antenna elements are placed at an optimized distance from each other with independent partial ground planes. The proposed design is also fabricated, and the measured results have been compared with those obtained in a simulated environment. It has been observed that both results are quite promising and well-comparable. The size of the proposed design is about (28 × 28) cm^2 as the first resonating frequency is 0.9 GHz. Nevertheless, the proposed design is suitable to integrate on the rooftop of the modern passenger cars with 5G automotive wireless applications.

***Index Terms*—**5G, antennas, automotive, multi-input-multi-output (MIMO), sub-6 GHz

I. INTRODUCTION

Due to the vast advancements in the field of wireless communication, various application scenarios such as low bandwidth, complex systems, limited channel capacity, and low data rates present challenges for effective communication systems [1, 2]. Therefore, over the past few years, the development of next-generation (5G and 6G) communication systems at sub-6 GHz, mmWave, and sub-THz frequency bands has featured higher channel capacity and enhanced data rates, ensuring the reliability and effectiveness of the transmitted or received signal [3-5]. There are two frequency bands that have been considered worldwide for next-generation wireless communication systems: one is sub-6 GHz, i.e., the lower frequency band (below 6 GHz), and the second one is mmWave which includes frequencies either above 27 GHz or between 24 and 27 GHz [6]. However, certain issues related to the higher frequency of operations, such as signal path loss, as free space path loss is directly related to the frequency of operation, atmospheric attenuation, and signal fading correspondingly degrade the data rate according to standard link budget calculations [7, 8]. Moreover, the problem becomes more severe when a single antenna element is used, as it has limited gain. Therefore, to address these issues, the sub-6 GHz frequency band and the multi-input multi-output (MIMO) antenna system are in greater demand among commercial and automotive use cases [9-11]. MIMO antenna systems are utilized in modern wireless communication, especially for long-term evolution (LTE), 5G, and 6G. The MIMO system consists of multiple antenna elements arranged in different configurations according to the use cases and it significantly impacts enhancing the spectral efficiency, improving channel capacity by utilizing the same spectrum, and reducing transmitted power. With all these factors, MIMO systems are

of frequencies with appropriate gain and diversity parameters analysis. Therefore, the proposed design can be considered for practical automotive applications. Some of the following key novelty parameters are as follows: 1. Frequency: 0.7 GHz - 5.5 GHz (dedicated for 5G automotive wireless applications) 2. Impedance bandwidth – 4800 MHz 3. Peak Gain – 8.8 dB 4. MIMO Analysis of all the diversity parameters.

more capable of delivering high data rates in densely populated areas. However, a high mutual coupling coefficient becomes a key challenge while designing such a system, as the antenna elements are closely packed on the chip. Therefore, various research articles have been published in recent years to deal with this situation, and various techniques have been adapted to minimize the inter-element isolation. The presented articles propose different configurations with defective ground structures, slotted patches, multilayer substrate structures, spider-shaped structures, flexible material antennas, etc., depending on the use case. Such designs have been elaborated in the next section.

II. LITERATURE SURVEY

For instance, a low-profile 4-element ultra-wideband antenna is presented with a modified substrate and a defected ground structure providing isolation < −16 dB between radiating elements. However, the structure faces challenges while fabricating with modified substrate [12]. In another paper, a four-element MIMO antenna design for mmWave applications is presented with wideband and high gain characteristics. However, the implemented defective ground structure is complex in nature [13]. A low-frequency 4-port MIMO antenna is designed with excellent impedance matching and isolation in the required band of frequencies [14]. In another work, a compact four-element design is presented for sub-6 GHz in which two elements are of the same type and the other is only quarter wavelength microstrip slot antennae. The paper consists of all the required parameters but still missing some of the significant MIMO evaluation parameters [15]. Two octagonal elements are arranged in MIMO configuration with defected ground structure to ensure impedance matching and isolation in C-band applications. The analysis of MIMO specifications has been rigorously done without any information on channel capacity loss [16]. A flexible wideband MIMO antenna is designed on flexible conductive material along with a partial ground plane. The authors explained the envelope correlation coefficient (ECC) without mentioning the other parameters [17]. A spider-shaped fractal MIMO antenna is discussed and analyzed on the basis of S-parameters along with the specific absorption rate without any discussion of channel capacity loss [18]. In another article, the authors present the development of a semi-circular corner cut MIMO antenna with a defected ground structure (DGS), designed for 5G-Advanced and 6G automotive applications [19]. Similarly, a fractal 1×2 MIMO antenna design with a DGS for sub-6 GHz 5G automotive applications has been presented. It operates at multiple frequencies (0.7, 2.6, 3.1, 3.5 GHz), achieves up to 12.9 dBi gain, and exhibits low mutual coupling (≤ −50 dB), making it suitable for integration into car body components for reliable high-data-rate communication [20, 21]. In recent years, numerous antenna designs have been proposed for sub-6 GHz 5G applications, especially targeting automotive environments. Prior studies have established the effectiveness of MIMO (Multi-Input Multi-Output) configurations in enhancing channel capacity and reliability for vehicular communication. Antennas operating in the sub-6 GHz spectrum are particularly important due to their favorable propagation characteristics and compatibility with existing infrastructure.

In this paper, four-element semi-circular arc-slotted antenna element is arranged into MIMO configuration with the addition of a partial ground plane. The proposed antenna is capable of operating in the sub-6 GHz frequency band covering n1, n3, n8, n41, n77, and n78 specifically for 5G satellite applications.

The proposed design exhibits the wide bandwidth covering the very low band of frequencies with appropriate gain and diversity parameters analysis. Therefore, the proposed design can be considered for practical automotive applications. Some of the following key novelty parameters are as follows: 1. Frequency: 0.7 GHz - 5.5 GHz (dedicated for 5G automotive wireless applications) 2. Impedance bandwidth – 4800 MHz 3. Peak Gain – 8.8 dB 4. MIMO Analysis of all the diversity parameters

III. DESIGN CONSIDERATIONS AND ANALYSIS OF PROPOSED ANTENNA

The proposed antenna begins with the design of a microstrip fed circular patch antenna on the low-cost substrate material. The proposed design is printed on FR4 substrate material having $\varepsilon_r = 4.4$, $h = 1.57$ mm and $\tan\delta = 0.02$. As the antenna is designed for very low frequency i.e., $f_r = 0.7$ GHz, the radius of the antenna is calculated using (1) and (2) [22, 23], as $a_r = 32$ mm.

- The radius of the circular patch of the single antenna at the lowest resonating frequency, which is fr = 0.8 GHz.

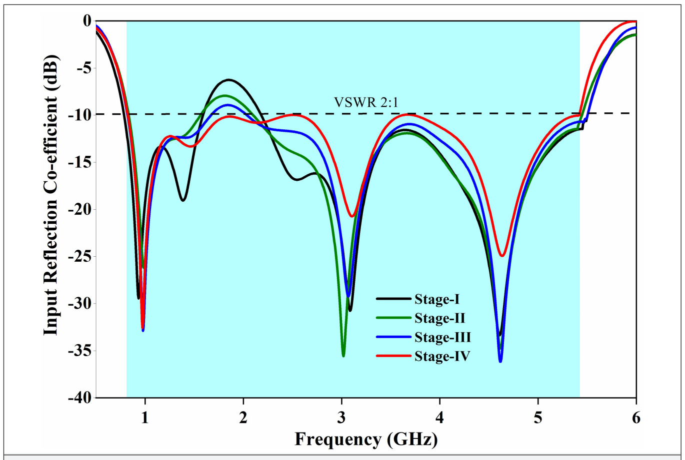

Fig. 1. Input reflection coefficient of the proposed design at different stages.

$$a = \frac{F}{\sqrt{1 + \frac{2h}{\pi \varepsilon_r F\left[ln\left(\frac{F\pi}{2h}\right) + 1.7726\right]}}} \quad Where\ F\ \frac{8.791 \times 10^9}{f_r\sqrt{\varepsilon_r}} \tag{1}$$

- The stage wise performance of the design and proposed design is shown in Fig. 1 and B and Fig. 2 respectively, so as to achieve the desired bandwidth.
- The width of the feed line (FW) was calculated according to the equation mentioned below; however, some parametric analyses were also performed as presented in Fig. 5C to investigate the impact of feed width on antenna bandwidth, in order to achieve desired results for a single antenna.

$$F_W = \frac{7.48h}{e^{\left(z_0 \frac{\sqrt{\varepsilon_r + 1.41}}{87}\right)}} - 1.25t \tag{2}$$

Where h = Height of substrate.

t = Thickness of metal.

z_0 = impedance of feed line as 50Ω.

Further modifications are performed on the conventional circular patch antenna. For instance, in the first stage, a semi-circular shape is etched from the top of the patch element, and in the final stage, two more semi-circular cuts are provided at both side edges of the design, as illustrated in Fig. 3. The dimensional pictorial view along with their corresponding parameters is shown in Fig. 4 and the dimensional parameters are illustrated in Table I. CST Microwave

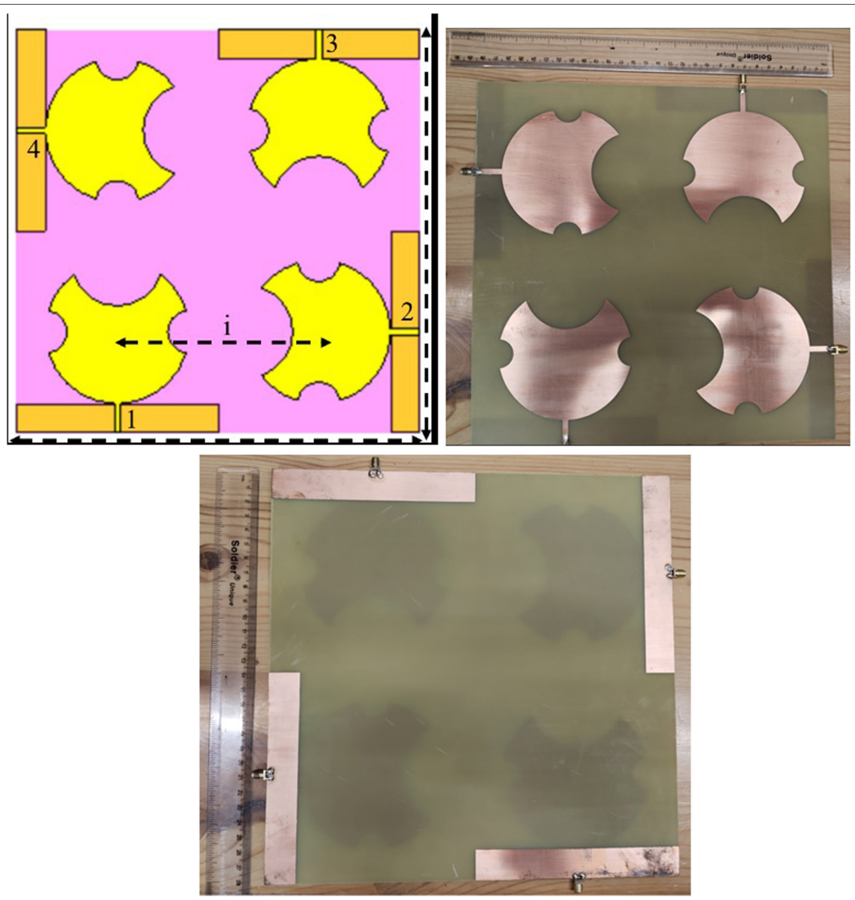

Fig. 2. Proposed multi-input-multi-output antenna. (A) Simulated design, (B) top view of fabricated prototype, and (C) bottom view of fabricated prototype.

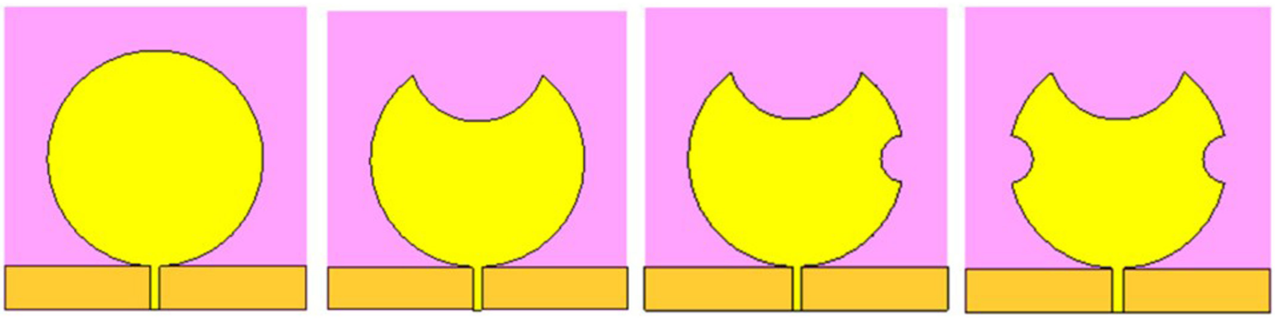

Fig. 3. Evolution stages of proposed single-element antenna. (A) Conventional circular patch, (B) first stage, (C) second stage, and (D) final stage.

Studio has been used for the simulation purpose of the proposed single element and MIMO antenna.

The size of the ground plane plays a significant role in determining the performance of the antenna. Therefore, the full ground plane has been modified into a partial ground plane to achieve the −10 dB impedance matching covering sub-6 GHz frequencies. The conventional single-element patch antenna discussed in the previous section is utilized in designing a four-element MIMO antenna with an orthogonal configuration as shown in Fig. 2 (A). The top and bottom views of the fabricated prototype of the proposed design can be visualized in Figs. 2B and 2C respectively. In this figure, the antenna elements are arranged in an orthogonal position with an overall size of (28 × 28) cm^2 and the distance between the elements is approximately equal to half wavelength of the resonating frequency (i.e. i = 140 mm). Even though the size of the proposed design is large, it is still it is suitable to integrate on the rooftop of the modern passenger car.

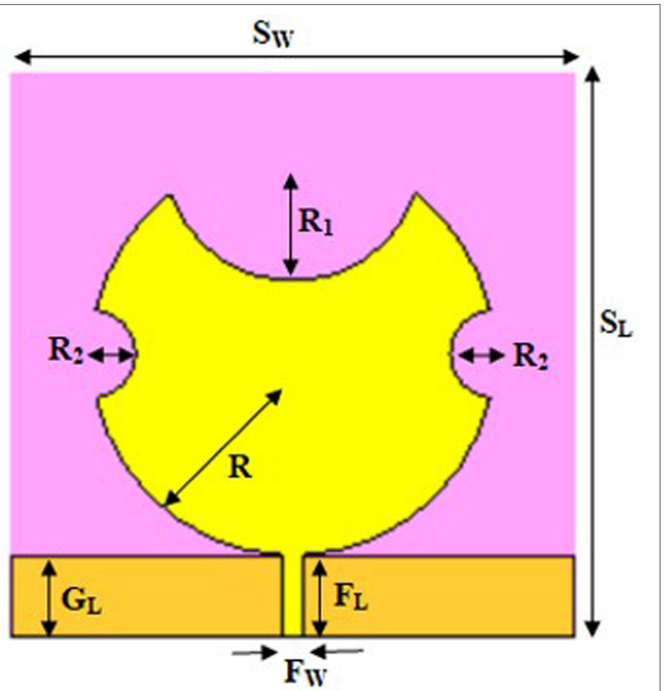

Fig. 4. Dimensional view of the proposed single-element antenna (SL = 140, SW = 140, FL = GL = 20, R = 50, R1 = 32, R2 = 11, FW = 4 (All values are in mm).

IV. RESULTS AND ANALYSIS OF PROPOSED MIMO ANTENNA

The parametric analysis with different ground lengths has been studied and illustrated in Fig. 5, which demonstrates that ground length, G_L = 20 mm is the optimum solution in which the antenna covers −10 dB impedance matching in the desired range of frequencies except for 1.6 GHz–2.2 GHz. The input reflection coefficient variations with respect to frequency of all the stages are shown in Fig. 5, which depicts that the final stage exhibits −10 dB impedance bandwidth in the entire sub-6 GHz band. This band majorly includes n40 (2300–2400 MHz), n41 (2496–2690 MHz), n46 (5150–5925 MHz), n77 (3300–4200 MHz), n79 (4400–5000 MHz). Further, it can be observed that all the stages except stage IV exhibit the notching in the frequency

TABLE I. DIMENSIONAL PARAMETERS OF SINGLE-ELEMENT ANTENNA AND MULTI-INPUT-MULTI-OUTPUT ANTENNA

Parameters	Values (mm)	Parameters	Values (mm)
$S_L = S_W$	140	F_W	4
R	50	F_L, G_L	20
R_1	32	h	280
R_2	11		

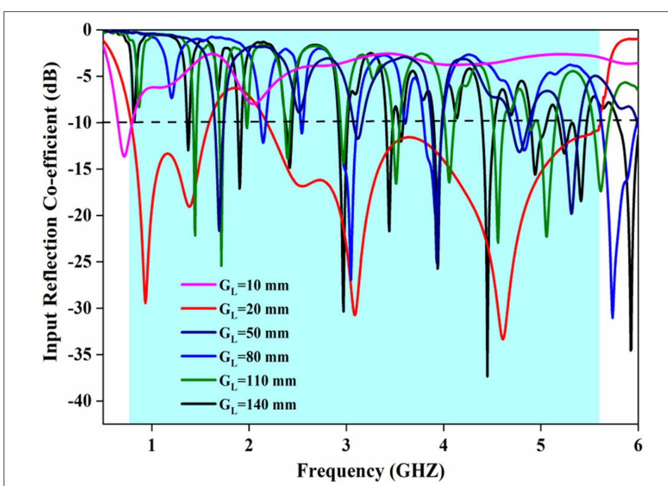

Fig. 5. Effect of ground plane length on input reflection coefficient (dB) of single-element circular patch antenna.

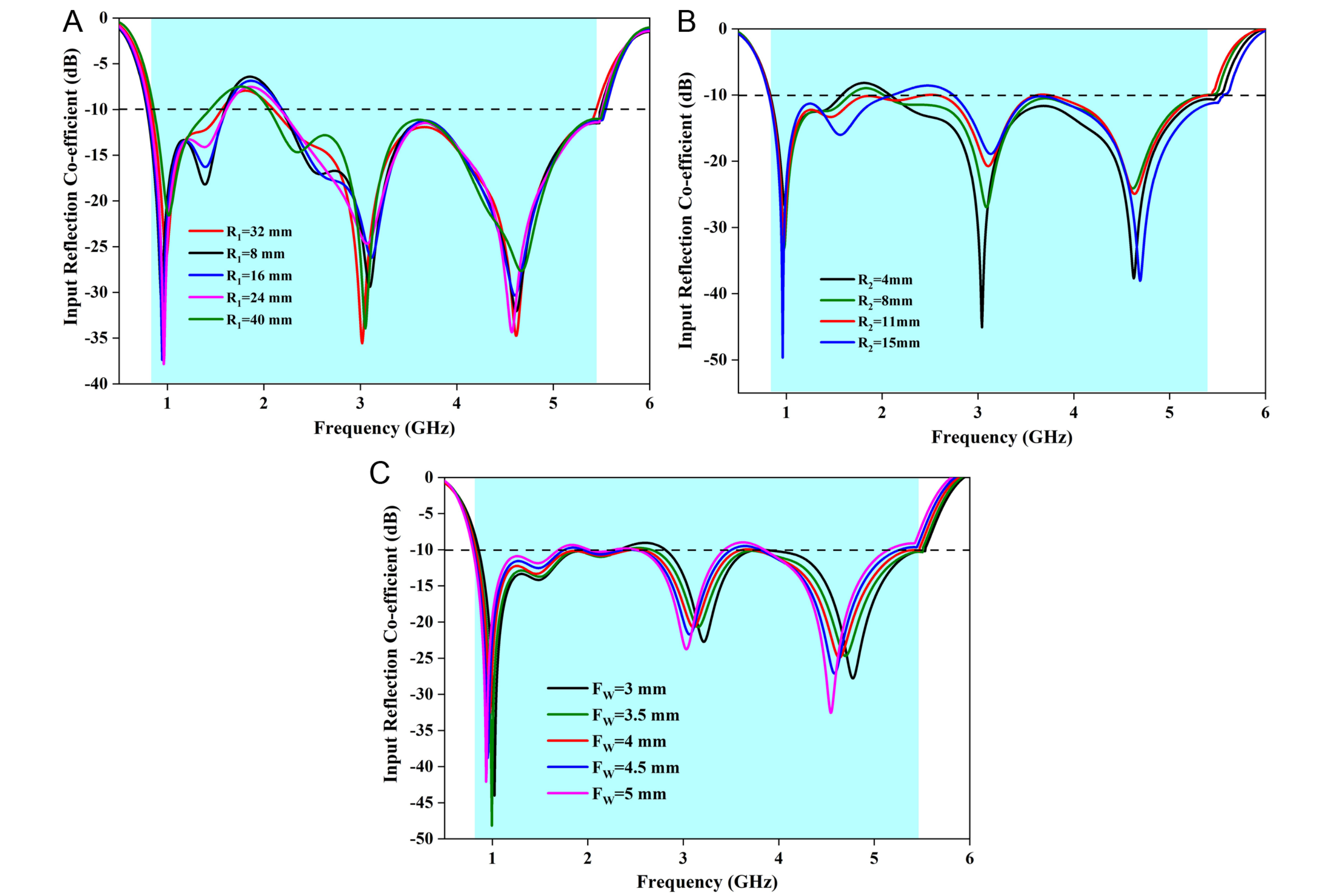

Fig. 6. Parametric analysis of dimensional specifications. (A) Radius of top cut (R1), (B) radius of side cuts (R2), and (C) feed line width (FW).

range of about 1.6–1.7 GHz. However, stage IV achieves the entire sub-6 GHz frequency band with −10 dB impedance bandwidth.

There are various dimensions involved in the design process, and these dimensions have been calculated following the standard procedures. However, some of the parameters need to be optimized to achieve the required performance parameters for the intended use cases. Therefore, initially, the radii of three cuts have been considered for parametric analyses to achieve optimized desired results. Firstly, the radius of the top semi-circular cut (R_1) is considered for analysis, and the corresponding input reflection coefficient variations have been shown in Fig. 6A, it can be illustrated that there is still there is a discrepancy in achieving the input reflection coefficient near 1.8 GHz. For further improvement, the size of the side cuts is also optimized, and the corresponding reflection coefficient plot is shown in Fig. 6B. Radius of side cuts, i.e., $R_2 = 11$ mm is chosen as the best choice, which provides excellent impedance matching across the entire band of sub-6 GHz. Finally, impedance matching is further optimized by choosing the appropriate width of the feed line (F_W) which directly impacts the impedance matching between the patch edge and the 50 Ω port, and the analysis is shown in Fig. 6C. It can be observed that there is only a variation in the value of S_{11}(dB) which satisfies all the bandwidth requirements, with the variation in feed width, and a value of 4 mm is chosen as the best one.

The simulated and measured S_{11}(dB) comparison is illustrated in Fig. 7A. Both curves are in good agreement except for some shifting in frequency in the C-band and impedance mismatch at 4.7 GHz. This is due to the soldering the connectors and fabrication tolerances. Moreover, the mutual coupling [11, 24, 25] is well below -15 dB in the entire frequency range as the distance between the elements has been optimized as illustrated in Fig. 7B. The gain of the proposed MIMO antenna is obtained from the simulation and validated through measurement as depicted in Fig. 8. The gain values are obtained from 0.5 GHz to 6 GHz with a frequency gap of 0.275 GHz. The simulated gain curve shows that the antenna achieved a peak gain of 8.8 dB in the resonating band; however, the measured peak gain reduced to about 0.5 dB, also showing a good agreement between the curves, with nominal fluctuations in the gain values at different frequencies. Figure 8 also presents the radiation efficiency of the antenna and indicates permissible results in the desired band with maximum radiation of about 99%.

Further, the far field characteristics have been characterized on the basis of radiation patterns at resonating frequencies of 0.9 GHz, 3 GHz, and 4.7 GHz, which are illustrated in Fig. 9 and 3-D polar plots have been shown in Fig. 10. The shape of the radiation patterns can be confirmed from the current distributions shown in Fig. 11. At 0.9 GHz, the antenna exhibits three and two radiating lobes at Phi = 0^0

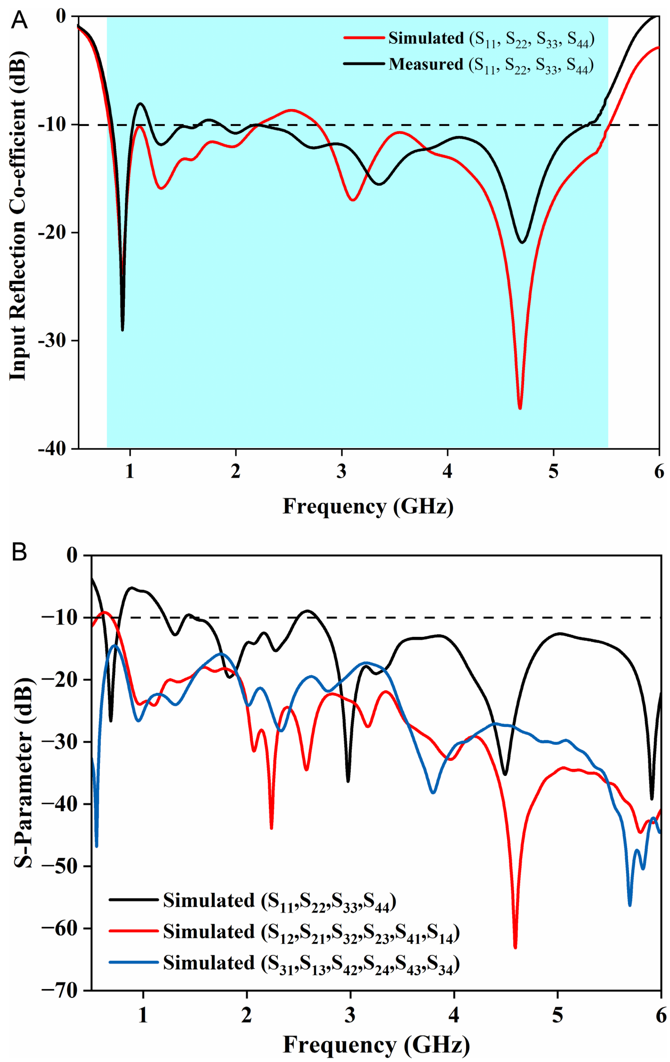

Fig. 7. S-parameters of the proposed multi-input-multi-output antenna design. (A) Simulated and measured S11 (dB) of the multi-input-multi-output design and (B) simulated isolation curve.

and Phi = 90⁰ respectively, having nearly equal radiated power in different directions of theta. However, at Phi = 0⁰, both simulated and measured results possess the main lobe direction at about 170⁰ with nearly the same magnitude of 2.31 dB and 3dB angular width of 51.4⁰. On the other hand, at Phi = 90⁰, the direction of the main lobe is in 160⁰ with magnitude and 3dB angular width of 2.59 dB and 91⁰ respectively. At 3 GHz, both simulated and measured radiation patterns agree well with slight power fluctuations at different angles of theta in Phi = 0⁰ and Phi = 90⁰ plots. Besides these, at Phi = 0⁰, the main lobe is directed towards 330⁰ with maximum lobe magnitude and 3dB angular width of 1.56 dB and 37.7⁰ respectively. Similarly at Phi = 90⁰, the main lobe magnitude and 3dB angular width of 1.45 dB and 64.2⁰, respectively, is directed along 41⁰. Further, the pattern at 3 GHz demonstrates the first higher-order mode as depicted in the current distribution Fig. 11 (B). In a similar manner, the radiation pattern characteristics of the antenna have been studied at 4.7 GHz and presented in Fig. 9C. In this case, both the simulated and measured field patterns concur at Phi = 0⁰ and Phi = 90⁰ with insignificant power

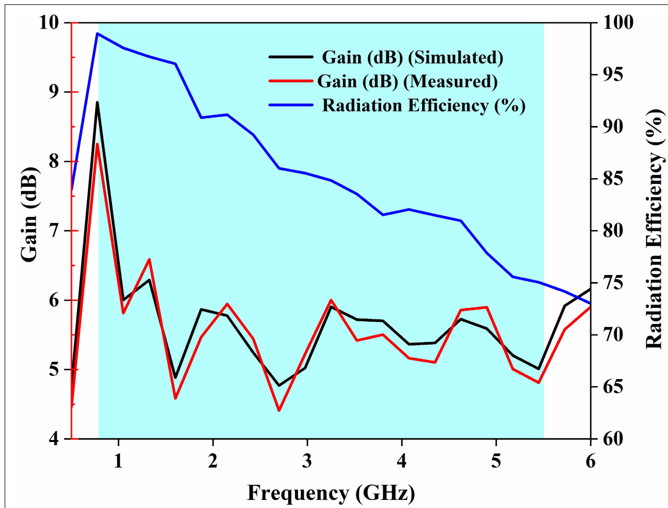

Fig. 8. Gain and radiation efficiency of the proposed multi-input-multi-output antenna.

variations at different angles of theta. In the field pattern at Phi = 0⁰, the main lobe is directed in 306⁰ with peak lobe magnitude and 3dB angular width of 3 dB and 86⁰ respectively. Whereas at Phi = 90⁰, the main lobe of magnitude 1.32 dB is directed along 331⁰ with a 3dB angular width of 22.6⁰. At last, the radiation pattern at 4.7 GHz exhibits two major lobes reflecting null in the broadside direction.

V. MULTI-INPUT-MULTI-OUTPUT DIVERSITY ANALYSIS

As the antenna is proposed for MIMO applications, it is of the utmost importance to assess the diversity performance as per methods suggested in [6] [26-28].

A. Envelope Correlation Coefficient

The ECC is the very first parameter for measuring the diversity performance of the MIMO antenna, and it can be evaluated from the S-parameters as expressed in (3).

$$ECC = \frac{\left|S_{mm}^{*}S_{mn} + S_{nm}^{*}S_{nn}\right|^{2}}{\left(1-\left|S_{mm}\right|^{2}-\left|S_{nm}\right|^{2}\right)\left(1-\left|S_{nn}\right|^{2}-\left|S_{mn}\right|^{2}\right)} \tag{3}$$

The ECC value should be of minimum value to establish the lowest correlation between the elements. The plot of the calculated ECC with respect to frequency is shown in Fig. 12.

B. Directive Gain

Directive gain (DG) establishes the relationship between transmission power loss when different varieties of schemes are applied to the system and it is expressed in (4). Figure 13 illustrates the DG to be almost 10 dB in the frequency band of interest.

$$DG = 10\sqrt{1-\left|ECC\right|^{2}} \tag{4}$$

VI. Comparison With Related Work

The proposed antenna and its corresponding parameters are compared with other related work, as illustrated in Table II. It can be

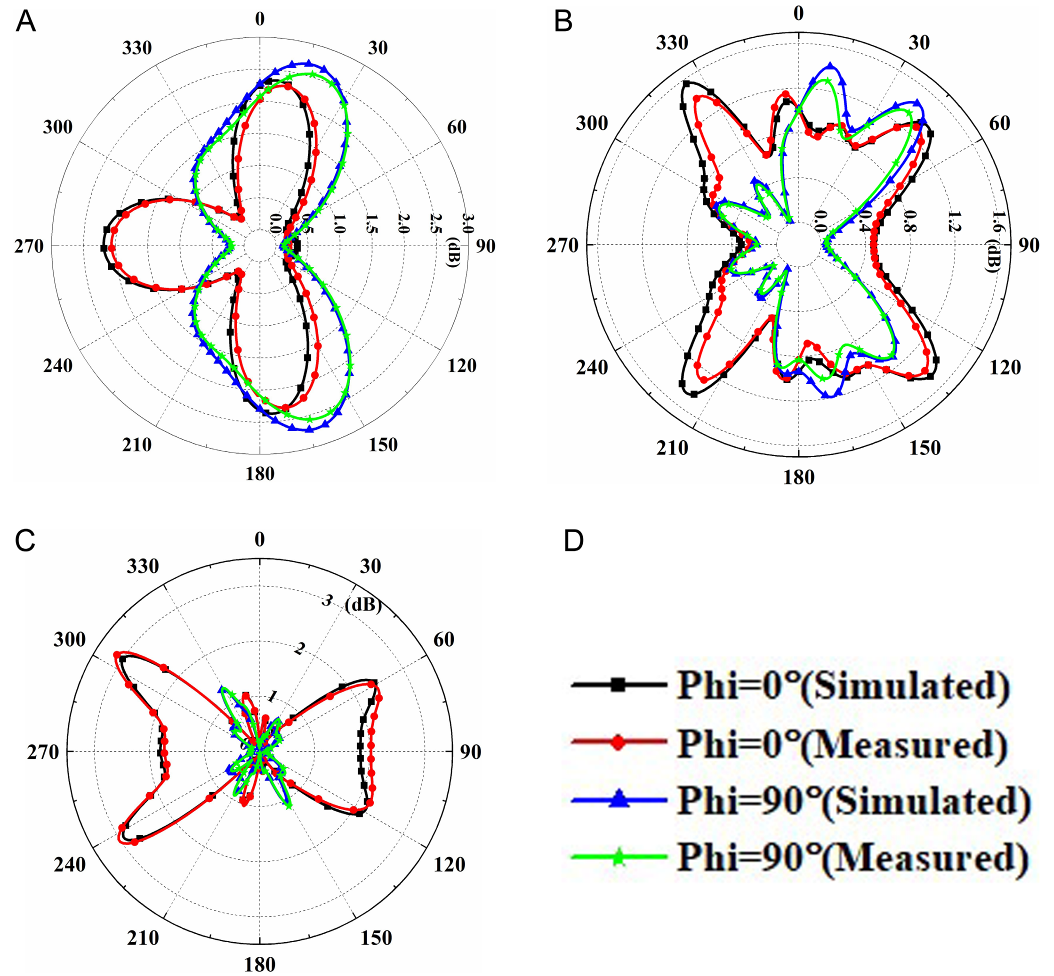

Fig. 9. Radiation patterns of the proposed multi-input-multi-output antenna design at (A) 0.9 GHz, (B) 3 GHz, and (C) 4.7 GHz.

observed that the proposed design is able to resonate at sub-6 GHz covering n1, n3, n8, n41, n77, and n78 specifically for 5G satellite applications [29-30]. Even though the proposed design possesses a higher electrical size compared to (12), (16), (17), and (18), it exhibits superior characteristics either in terms of impedance bandwidth, gain, or gain or use of a number of radiating elements. On the other hand, (13) and (28) have higher electrical sizes than this proposed work; however, they exhibit lower impedance bandwidth and gain. While considering the use of the same number of radiating elements along with their corresponding results, this work possesses superior impedance bandwidth and gain in comparison to (13) and (17). Further, considering the achieved gain in the resonating band, the proposed design shows a superior gain value compared to others reported, even using more radiating elements (12). Furthermore, it can be said that the proposed design exhibits a wide bandwidth covering the very low band of frequencies with appropriate gain and diversity parameter analysis. Therefore, the proposed design can be considered for practical automotive applications.

VII. CONCLUSION

This article presents a MIMO-configured antenna composed of four radiating elements embedded with a variety of semi-circular cuts with an independent partial ground plane. The proposed antenna design covers the frequency bands that are included in the sub-6 GHz. The resonance peaks in the bandwidth have been achieved at 0.9 GHz, 3 GHz, and 4.7 GHz with a peak gain of 8.8 dB. The size of the antenna is large in terms of conventional scale but comparable in terms of wavelength. Still, the fabricated design is suitable for integration on the rooftop of the automobile, which can be utilized for communication with low earth satellites, and this type of communication is useful for various 5G automotive applications considered in the sub-6 GHz frequency bands. The future work of this article advances into the real-time integration in car parts and evaluates the performance of the antenna along with the added feature of circular polarization, which can be further utilized to minimize polarization losses and enhance the overall data rate according to link budget calculations.

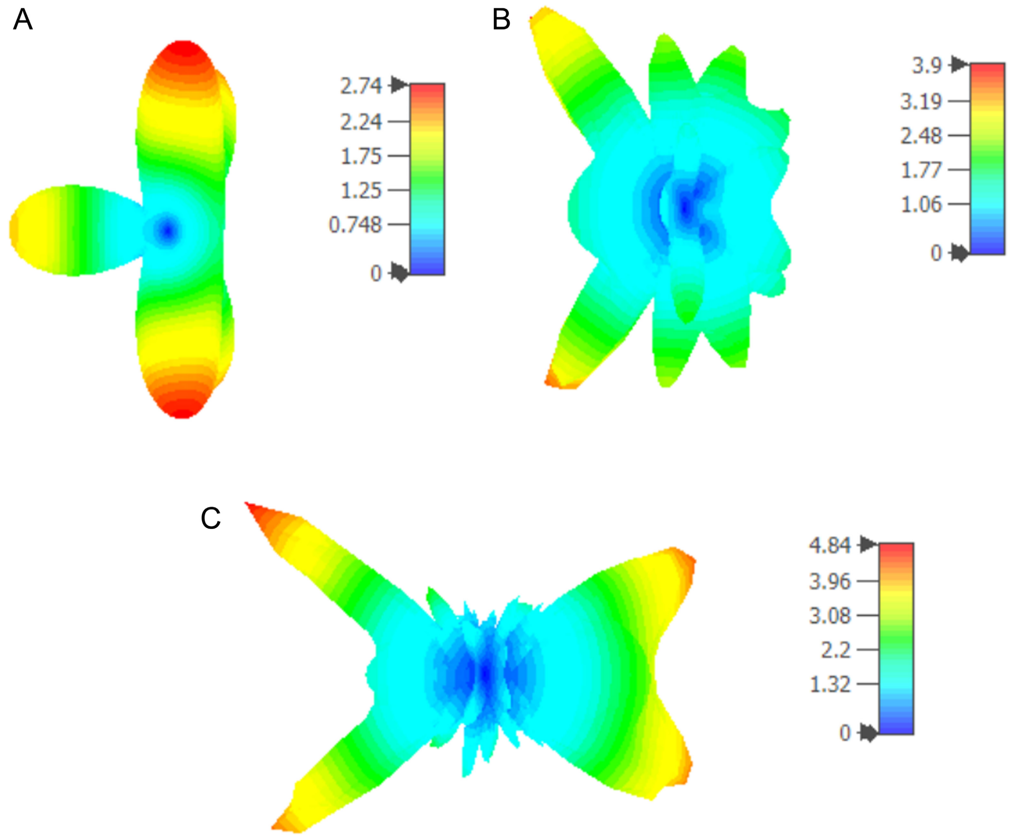

Fig. 10. 3D polar plots of the proposed multi-input-multi-output antenna design at (A) 0.9 GHz, (B) 3 GHz, and (C) 4.7 GHz.

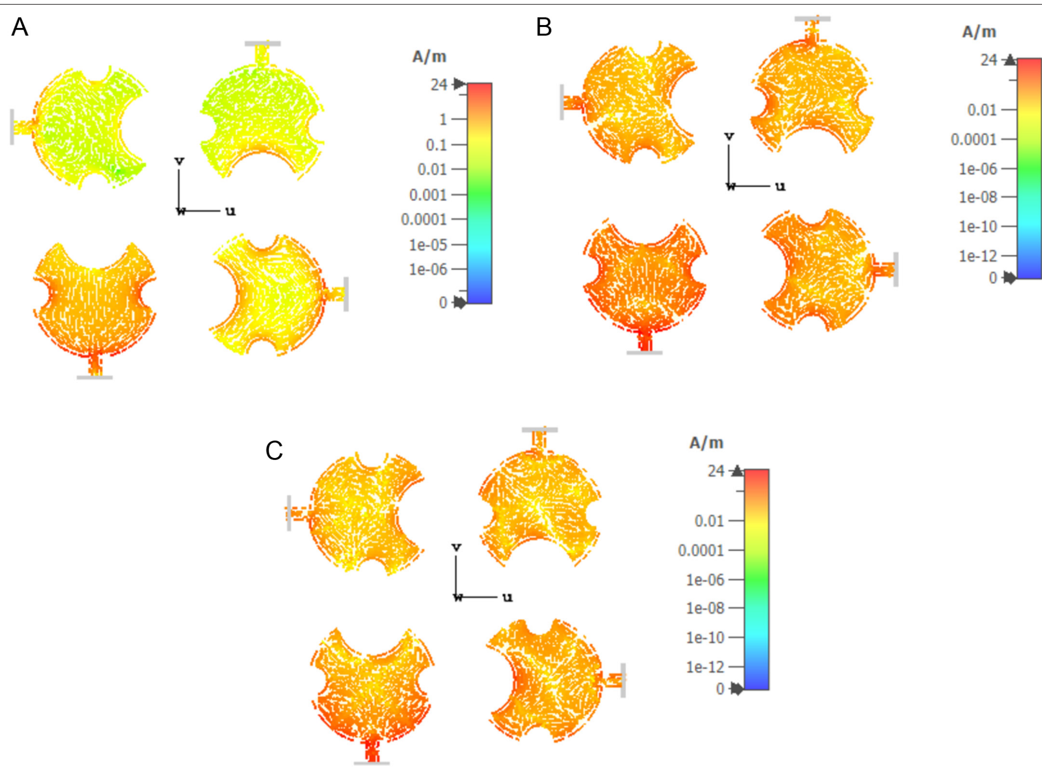

Fig. 11. Current distribution of the proposed multi-input-multi-output antenna at (A) 0.9 GHz, (B) 3 GHz, and (C) 4.7 GHz.

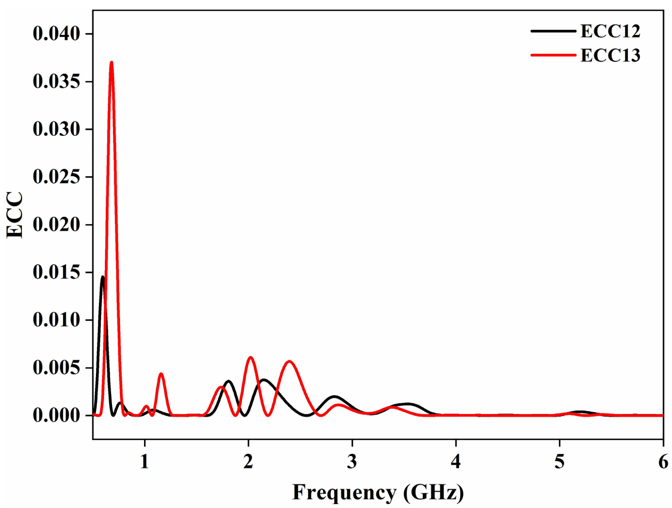

Fig. 12. Envelope correlation coefficient plot with frequency.

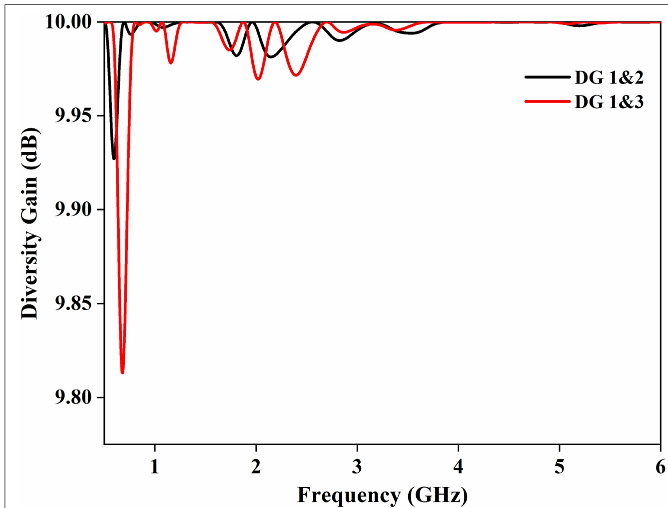

Fig. 13. Diversity gain plot with frequency.

TABLE II. COMPARATIVE ANALYSIS OF THE PROPOSED ANTENNA DESIGN WITH RELATED WORK

Reference	Resonating Frequency Band (GHz)	Size (mm³)	Isolation (dB)	Number of Antenna Elements	Max. Impedance Bandwidth (MHz)	Gain (dB)	Diversity Parameters
(12)	2.84–11	0.61λ × 0.61λ (90 × 90 × 1.6)	>15	8	8160	4.5	Yes
(13)	25.5–29.6	2.8λ × 3.26λ (30 × 35 × 0.76)	−17	4	4100	8.3	Yes
(16)	3.1–10.6	0.68λ × 0.8λ (30 × 40 × 0.8)	<−15	2	7500	8	Yes
(17)	2.21–6	0.33λ × 0.48λ (66 × 45 × 0.635)	>15	4	3790	0.53	Yes
(18)	2.24–2.5 3.6–3.99 4.4–4.6 5.71–5.9	0.308λ × 0.46λ (37 × 56 × 1.6)	≤−30	2	399	2	Yes
(31)	25.5–30	1.9λ × 1.12λ (20.5 × 12 × 0.79)	<−40	2	4500	8.75	No
Proposed Work	0.7–5.5	0.84λ × 0.84λ (280 × 280 × 1.57)	<−45	4	4800	8.8	Yes

Data Availability Statement: The data that support the findings of this study are available on request from the corresponding author.

Peer-review: Externally peer-reviewed.

Author Contributions: Concept – A.K.; Design – B.C.S.; Supervision – G.S.; Resources – S.R.M.; Materials – B.C.S.; Data Collection and/or Processing – B.C.S., S.R.M.; Analysis and/or Interpretation – B.C.S., S.R.M.; Literature Search – A.K., B.C.S., S.R.M.; Writing Manuscript – A.K., B.C.S.; Critical Review – A.S., R.K.; Other – A.S., R.K.

Declaration of Interests: The authors have no conflict of interest to declare.

Funding: The authors declared that this study has received no financial support.

REFERENCES

1. M. Sharma et al, "Conformal ultra-compact narrowband 60.0 GHz four-port millimeter wave MIMO antenna for wearable short-range 5G application," *Wirel. Netw.* [Internet], vol. 30, no. 3, pp. 1815–1831, 2024. [CrossRef]
2. P. Tiwari, V. Gahlaut, M. Kaushik, P. Rani, A. Shastri, and B. Singh, "Advancing 5G connectivity: A comprehensive review of MIMO antennas for 5G applications," *International Journal of Antennas and Propagation*, vol. 2023, 19pp, 2023. [CrossRef]

3. V. Kikan, T. Bano, B. S. Neha, A. Kumar, and M. Sharma, "A comparative review on theory and designing of 28/38GHz 5G MIMO and array antenna," In *Proc. IEEE* International Conference on Innovative Data Communication Technologies and Application, ICIDCA 2023, pp. 1014–1020, 2023.
4. C. -N. Hu, and D. -C. Chang, "Millimeter- Wave (mmW) Antenna Design for 5G Massive MIMO applications," in *Cross Strait Quad-Regional Radio Science and Wireless Technology Conference (CSQRWC)*. Xuzhou, China: IEEE, 2018, pp. 1–3. [CrossRef]
5. A. Kumar, H. -P. Petry, U. Tayyab, and M. A. Hein, "Link budget considerations for automotive 5G LEO satellite-based communications," IEEE USNC-URSI Radio Science Meeting (Joint with AP-S Symposium), Denver, CO, USA, 2022, pp. 106–107. [CrossRef]
6. T. Addepalli, M. Sharma, M. S. Kumar, G. Naveen Kumar, P. R. Kapula, and C. M. Kumar, "Self-isolated miniaturized four-port multiband 5G sub 6 GHz MIMO antenna exclusively for n77/n78 & n79 wireless band applications," *Wirel. Netw.* [Internet], vol. 30, no. 2, pp. 1037–1053, 2024. [CrossRef]
7. GPP, "TS 38.101–4," *Technical Specifications Group Radio Access Network;NR; User Equipment (UE) Radio Transmissioon and Reception; Part 4:Performance Requirments* v, 17.3.0, 2022.
8. I. Elfergani, J. Rodriguez, A. Iqbal, M. Sajedin, C. Zebiri, and R. A. AbdAlhameed, "Compact millimeter-wave MIMO antenna for 5G applications," 14th European Conference on Antennas and Propagation (EuCAP), Copenhagen, Denmark, 2020, pp. 1–5. [CrossRef]
9. M. S. Sharawi, "Current misuses and future prospects for printed multiple-input, multiple-output antenna systems [wireless corner]," *IEEE Antennas Propag. Mag.*, vol. 59, no. 2; pp. 162–170, 2017. [CrossRef]
10. U. Tayyab, A. Kumar, H. -P. Petry, M. G. Robbani, T. Wack, and M. A. Hein, "Circularly polarized patch antenna array for 5G automotive satellite communications," 53rd European Microwave Conference (EuMC), Berlin, Germany, 2023, pp. 794–797. [CrossRef]
11. I. Nadeem, and D. -Y. Choi, "Study on mutual coupling reduction technique for MIMO antennas," in *IEEE Access*, vol. 7, pp. 563–586, 2019. [CrossRef]
12. T. Addepalli et al., "8-port semi-circular arc Mimo antenna with an inverted L-strip loaded connected ground for Uwb applications," *Electronics*, vol. 10, no. 12, pp. 1–19, 2021. [CrossRef]
13. M. Khalid et al., "4-port MIMO antenna with defected ground structure for 5G millimeter wave applications. Electron.," vol. 9, no. 1, pp. 1–13, 2020.
14. D. Sarkar, and K. V. Srivastava, "A compact four-Element MIMO / diversity antenna with enhanced bandwidth," *Antennas Wirel. Propag. Lett.*, vol. 16, pp. 2469–2472, 2017. [CrossRef]
15. H. Li, J. Xiong, and S. He, "A compact planar MIMO antenna system of four elements with similar radiation characteristics and isolation structure," *IEEE Antennas Wirel. Propag. Lett.*, vol. 8, pp. 1107–1110, 2009. [CrossRef]
16. T. C. Tang, and K. H. Lin, "An ultrawideband MIMO antenna with dual band-notched function," *IEEE Antennas Wirel. Propag. Lett.*, vol. 13, pp. 1076–1079, 2014. [CrossRef]
17. A. Desai, M. Palandoken, J. Kulkarni, G. Byun, and T. K. Nguyen, "Wideband flexible/transparent connected-ground MIMO antennas for Sub-6 GHz 5G and WLAN applications," *IEEE Access*, vol. 9, pp. 147003–147015, 2021. [CrossRef]
18. S. Chouhan, D. Kumar, V. Singh, and S. Singhal, "Spider-shaped fractal MIMO antenna for WLAN / WiMAX / wi-fi / Bluetooth / C-band applications," *AEUE Int. J. Electron. Commun.* [Internet], vol. 110, 152871, 2019. [CrossRef]
19. A. Kumar, A. Kumar, and A. J. A. Al-Gubari, "Development of semi-circular corner cut MIMO antenna for 5G-advanced and 6G automotive wireless applications," *Results Eng.*, vol. 25, 2025. [CrossRef]
20. A. Kumar, G. Singh, M. K. Abdulhameed, S. R. Hashim, and A. J. A. Al-Gburi, "Development of Fractal 5G MIMO antenna for sub 6 GHz wireless automotive applications," *Prog. Electromagn. Res. M*, vol. 130, pp. 121–128, 2024. [CrossRef]
21. R. K. Mistri et al., "Quad Element MIMO antenna for C, X, Ku, and ka-band applications," *Sensors (Basel)*, vol. 23, no. 20, p. 8563, 2023. [CrossRef]
22. C. A. Balanis, "Antenna theory: Analysis and design" [Internet], 2005, *Amazon*, 1136pp. Available: http://www.amazon.com/Antenna-Theory-Analysis-Design-Edition/dp/047166782X.
23. P. Gupta, L. Malviya, and S. V. Charhate, 5G multi-element/port antenna design for wireless applications:a review. *Int. J. Microw. Wirel. Technol*, pp. 1–21, 2019.
24. U. Tayyab, A. Kumar, H.-P. Petry, M. E. Asghar, and M. A. Hein, "Dual-band nested circularly polarized antenna array for 5G automotive satellite communications," *Appl. Sci.*, vol. 13, no. 21, 11915, 2023. [CrossRef]
25. M. A. Abdalla, and A. A. Ibrahim, "Compact and closely spaced metamaterial MIMO antenna with high isolation for wireless applications," in *IEEE Antennas Wirel. Propag. Lett.*, vol. 12, pp. 1452–1455, 2013. [CrossRef]
26. S. Bao, W. Ren, Q. Zeng, Z. Xue, and W. Li, "An ultra-wideband multiple-input multiple-output antenna with dual band-notched characteristics," *Int. J. RF Microw. Comput. Aid. Eng.*, vol. 32, No. 2, e22979, 2022. [CrossRef]
27. A. Kumar, S. Anand, R. P. Choudhary, G. Singh, and A. Kumar, "Design of 8×8 phased array antenna for Sub-6 GHz 5G automotive wireless communications," 11th International Conference on Signal Processing and Integrated Networks (SPIN), Noida, India, 2024, pp. 123–127. [CrossRef]
28. W. A. Awan, T. Islam, F. N Alsunaydih, F. Alsaleem, and K. Alhassoon, "Correction: Dual-band MIMO antenna with low mutual coupling for 2.4/5.8 GHz communication and wearable technologies," *PLoS One*, e0305186, 2024. [CrossRef] Correction: "Correction: Dual-band MIMO antenna with low mutual coupling for 2.4/5.8 GHz communication and wearable technologies," *PLoS One*, vol. 19, no. 6, e0305186, 2024. (https://doi.org/10.1371/journal.pone.0305186)
29. 3GPP, "TS 38.101–4," *Technical Specifications Group Radio Access Network;NR; User Equipment (UE) Radio Transmission and Reception; Part 4:Performance Requirments* v, 17.3.0, 2022.
30. F. Taher et al, "Design and analysis of circular polarized two-port MIMO antennas with various antenna Element orientations," *Micromachines*, vol. 14, no. 2, pp. 1–15, 2023.

Dr. Ashish Kumar received his B.Tech in 2008 and M.Tech. in 2012 from Punjabi University, Patiala, Punjab, India, and Ph.D. in 2020 from Sant Longowal Institute of Engineering and Technology, Longowal, Sangrur, Punjab, India. Dr. Kumar has also worked as a Postdoctoral Research Associate at the Technical University, Ilmenau, Thuringia, Germany. Previously, he was a research associate in the Department of Computer Science and Engineering at the Indian institute of technology, Delhi (IIT-D), India. At present, he is working as an assistant professor at Chitkara University, Rajpura, Punjab, India. He has published various research articles in national and international journals/conferences. His research includes automotive antennas, substrate integrated waveguide antennas, reconfigurable patch antennas, fractal antennas, and MEMS design.

Dr. Gurmeet Singh is currently working as an Assistant Professor in the School of Computing Science and Engineering. He has a total of over 3 years of teaching and research experience. He has been associated with Galgotias University since 2022. He has completed his M.Tech and PhD from Sant Longowal Institute of Engineering and Technology (Deemed to be University, under MHRD, Govt. of India), Longowal, Sangrur, Punjab, India-148106, in Electronics and Communication Engineering. He has published 05 research papers in international journals and 11 papers in international/national conferences. His area of interest is microstrip antenna design.

Bikash Chandra Sahoo received his Bachelor's degree in Electronics and Telecommunication Engineering from IGIT, Sarang, Odisha, in 2015, and his Master's degree in Electronics and Communication Engineering from Sant Longowal Institute of Engineering and Technology (SLIET), Punjab, in 2018. He has been working as an assistant professor at IGIT, Sarang from last 5 years. His research interests are in the field of MIMO antenna, 5G antenna arrays and wearable antenna.

Soumya Ranjan Mishra received his Ph.D in Electronics and Telecommunication Engineering in 2021 from Veer Srendra Sai University of Technology, Burla, Sambalpur, Odisha. He is currently working as an Assistant Professor at Indira Gandhi Institute of Technology, sarang, Odisha. He is working in the area of compact filtenna circuits for 5G applications, 5G MIMO antennas and antenna arrays.

Dr. Ashutosh Sharma is a Distinguished Professor at the Business School, Henan University of Science and Technology. He is an outstanding scholar of Computer Networks, the Internet of Things (IoT), and e-business applications. He is also acting as an international consultant for research at development at SFU, Russia. He has presided over one project of the BRICS Multilateral (Brazil-Russia-India-China-South Africa) Project, and more than two projects at the university level. He has participated in many national and international conferences. He has published more than 62 academic papers in important core WoS-SCI and Scopus-indexed journals. He is also working as an expert in the review committee for doctoral degrees in various national and international universities. Main Research Areas: Computer Networks and its Applications, Reliability Engineering and Risk Management, Information management and systems, Network System and Security, Artificial Intelligence and Machine Learning

Dr. Rajeev Kumar received his B.Tech and M.Tech Degrees in Electronics and Communication Engineering from Kurukshetra University, Kurukshetra, India in 2008 and 2010, respectively. He completed his PhD degree in Electronics Engineering from Banasthali University, Rajasthan, India in 2017. He is currently working as an Associate Professor in Department of Electronics and Communication Engineering, Chitkara University Institute of Engineering and Technology, Chitkara University, Punjab, India. His research interests include Reconfigurable Antenna, Ultra-wideband antenna, Multiband Antennas, Smart and MIMO Antennas Systems, Internet of Things and AI/ML Applications. During his research, He has published more than 60 research papers in various reputed publishing houses like IEEE, Wiley, Elsevier, Taylor and Francis, Hindawi, PIERS, MDPI and many more. Dr. Kumar has been served as a reviewer for many publishing houses like Wiley, Elsevier, Taylor and Francis and PIERS, etc.